Implicit Solvent Model Studies of the Interactions of the Influenza Hemagglutinin Fusion Peptide with Lipid Bilayers

Dalit Bechor and Nir Ben-Tal
Department of Biochemistry, George S. Wise Faculty of Life Sciences, Tel Aviv University, Ramat Aviv 69978, Israel

ABSTRACT The "fusion peptide," a segment of ~20 residues of the influenza hemagglutinin (HA), is necessary and sufficient for HA-induced membrane fusion. We used mean-field calculations of the free energy of peptide-membrane association (ΔG_{tot}) to deduce the most probable orientation of the fusion peptide in the membrane. The main contributions to ΔG_{tot} are probably from the electrostatic (ΔG_{el}) and nonpolar (ΔG_{np}) components of the solvation free energy; these were calculated using continuum solvent models. The peptide was described in atomic detail and was modeled as an α-helix based on spectroscopic data. The membrane's hydrocarbon region was described as a structureless slab of nonpolar medium embedded in water. All the helix-membrane configurations, which were lower in ΔG_{tot} than the isolated helix in the aqueous phase, were in the same (wide) basin in configurational space. In each, the helix was horizontally adsorbed at the water-bilayer interface with its principal axis parallel to the membrane plane, its hydrophobic face dissolved in the bilayer, and its polar face in the water. The associated ΔG_{tot} value was ~−8 to −10 kcal/mol (depending on the rotameric state of one of the phenylalanine residues). In contrast, the ΔG_{tot} values associated with experimentally observed oblique orientations were found to be near zero, suggesting they are marginally stable at best. The theoretical model did not take into account the interactions of the polar headgroups with the peptide and peptide-induced membrane deformation effects. Either or both may overcompensate for the ΔG_{tot} difference between the horizontal and oblique orientations.

INTRODUCTION

The infection of a cell by a virus is a complicated multistage process during which the virus penetrates the host cell membrane (Bentz, 1993; Hernandez et al., 1996). Viral envelope glycoproteins ("fusion proteins") are essential for the infection of the host cell. The glycoproteins attach the virus to the host cell membrane and then mediate the fusion of the viral and cellular membranes. Fusion proteins from different viruses share some common features. First, all known fusion proteins are class I integral membrane glycoproteins, i.e., they have one transmembrane helix, and the majority of their mass resides on the extracellular side of the host cell. Second, many of them are synthesized as long precursors that require cleavage to become fusion-active. Third, they form a tight complex of two subunits and arrange themselves in highly ordered oligomers.

The infection mechanism of influenza has been well-studied (Bentz et al., 1993; Carr and Kim, 1993, 1994; Clague et al., 1993; Stegmann and Heleius, 1993; Wilschut and Born, 1993) and the hemagglutinin (HA) glycoprotein identified as the fusion protein. The three-dimensional (3D) structure of HA has been determined in three different forms of the protein: 1) a precursor (at neutral pH), referred to as HA0 (Chen et al., 1998); 2) the mature protein at neutral pH, referred to as BHA (Wilson et al., 1981); and 3) a proteolytically cleaved form of the mature protein at the acidic pH of fusion, referred to as TBHA2 (Bullough et al., 1994). The protein is trimeric in form and its scaffold contains an elongated coiled coil.

HA can infect only after the long precursor (HA0) of 550 residues is cleaved into two (disulfide-bonded) subunits, HA1 and HA2. The HA1 subunit (residues 1–328 of HA0) contains the receptor's binding site and the HA2 subunit (residues 330–550 of HA0) contains a conserved segment of ~20 amino acids in length, termed the "fusion peptide" because of its function. Infection begins with HA1 binding to target membranes through cellular sialic acid receptors. Then endocytosis occurs: the virus is captured inside an endosome and is inserted into the host cell. In the mildly acidic environment inside the endosome, HA undergoes dramatic conformational changes, during which the fusion peptide is ejected from the hydrophobic core of HA. These changes, and probably an interaction of the fusion peptide with the host cell membrane, result in fusion of the virus and host cell membranes and a release of the viral genome into the cytoplasm of the target (host) cell (reviewed by Durell et al., 1997).

The 20-amino acid hydrophobic N-terminal region of the HA2 subunit is highly conserved within the influenza virus family. Mutagenesis studies show the crucial role of the sequence of the fusion peptide in promoting membrane fusion (Durell et al., 1997; Gething et al., 1986; Harter et al., 1989; Steinhauer et al., 1995). Synthetic peptide analogs of the N-terminus of HA2 that are 20 to 36 residues long associate with lipid membranes and can also promote bilayer fusion (Lear and DeGrado, 1987; Takahashi, 1990). Because the fusion peptide is missing in the low-pH structure (TBHA2), its conformation during fusion remains un-

Received for publication 5 September 2000 and in final form 8 November 2000.

Address reprint requests to Dr. Nir Ben-Tal, Dept. of Biochemistry, Tel Aviv University, Ramat Aviv 69978, Israel. Tel.: 972-3-640-6709; Fax: 972-3-640-6834; E-mail: bental@ashtoret.tau.ac.il; web: http://ashtoret.tau.ac.il.

© 2001 by the Biophysical Society

0006-3495/01/02/643/13 $2.00

known. However, with one exception (Gray et al., 1996), the available spectroscopic data suggest that it adopts a helical structure, especially when membrane-associated (Brasseur et al., 1990; Luneberg et al., 1995; Macosko et al., 1997; Takahashi, 1990). A helical wheel projection of the fusion peptide reveals its amphipathic nature and suggests that it is likely to be adsorbed onto membrane surfaces (White, 1992).

Several studies have been carried out to detect the orientation of the fusion peptide in lipid membranes. Measurements using spin-labeling EPR techniques that have been carried out using the 20 (Luneberg et al., 1995) and the 175 (Macosko et al., 1997) N-terminal residues of HA2 indicate that the fusion peptide inserts into lipid membranes in α-helix conformation and in an oblique orientation with an angle of between 25° and 45° from the membrane plane. In such orientation, the hydrophobic patch near the N-terminus of the peptide (Fig. 1 *A*, *upper white patch*) may be in contact with the hydrocarbon core of the bilayer, while the rest of the peptide is still in the water-membrane interface. This observation was recently verified using circular dichroism (CD) and attenuated total reflection-Fourier transform infrared (ATR-FTIR) techniques; a peptide corresponding to the 23 N-terminal residues of HA2 was observed at an angle of ~30° with respect to the membrane plane (Han et al., 1999). These studies suggest that the N-terminus of the fusion peptide is buried in the hydrocarbon region of the membrane (e.g., Luneberg et al., 1995, Fig. 9). Studies from many labs indicate that such an orientation of the N-terminus involves a large electrostatic desolvation free energy penalty of removing unsatisfied backbone hydrogen-bonded groups at the N-terminus from water into the hydrocarbon region of the bilayer (Kessel and Ben-Tal, 2000; White and Wimley, 1999). Indeed, very recent ^{15}N-NMR studies of the 20 N-terminal residues of HA2 suggest that the fusion peptide is at oblique orientations, but that it does not significantly penetrate into the hydrocarbon region of the bilayer (Zhou et al., 2000). According to these recent studies, the N-terminal amide group of the fusion peptide is protonated and is located close to the aqueous phase. Clearly, this subject requires further investigation.

Recently, Efremov et al. (1999b) carried out Monte Carlo simulations of the HA2(1–20) fusion peptide and its analogs in lipid bilayers. The peptides were represented in atomic detail and the simulations were carried out using a force field that takes into account van der Waals and electrostatic (using a distance-dependent dielectric constant) interactions, and torsion and hydrogen-bonding effects (Ne'methy et al., 1983). The lipid bilayer was represented by a two-phase slab model, in which one phase represents the hydrocarbon region and another (more polar) represents the polar headgroup region. A set of experimentally derived atomic solvation parameters (Efremov et al., 1999a) was used to calculate the desolvation effects associated with the transfer of the peptide from the aqueous phase into the headgroup and the hydrocarbon regions of the bilayer. The results of the simulations showed that the lipid bilayer enhances helix formation both in HA2(1–20) and in all of its analogs. In all the lowest energy states HA2(1–20) was, in essence, in α-helix conformation and was adsorbed on the bilayer in oblique orientation with its N-terminus immersed in the hydrocarbon region of the membrane, in close agreement

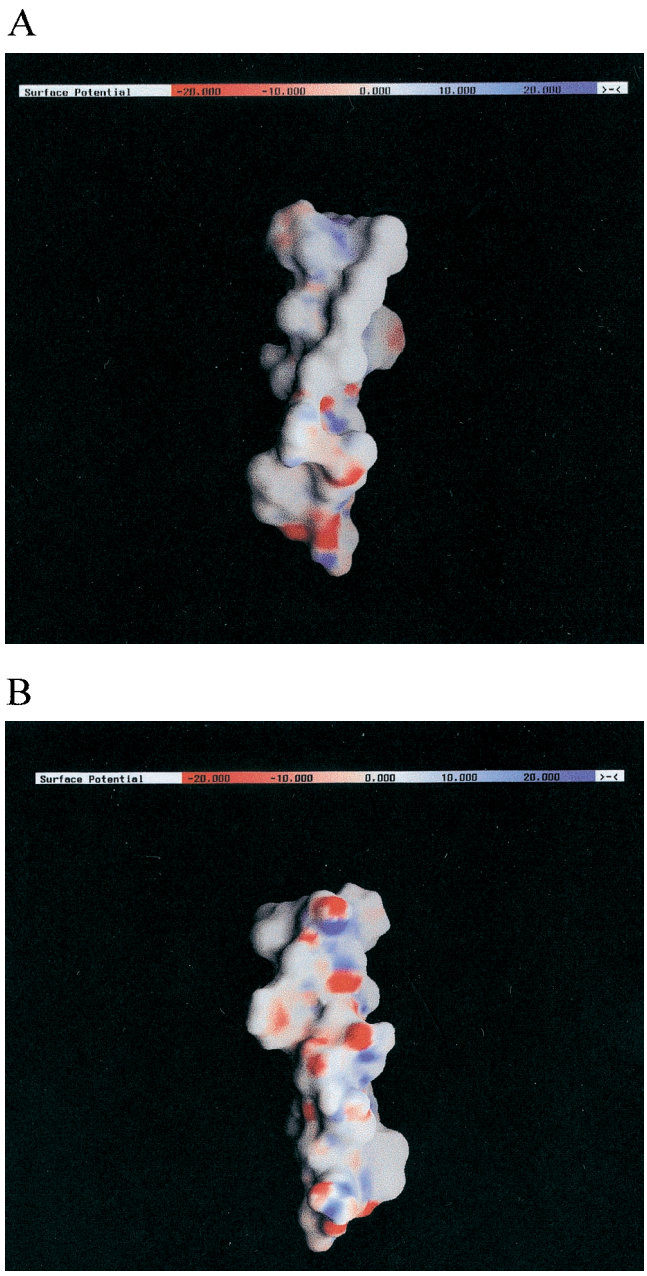

FIGURE 1 Electrostatic surface potential of HA2(1–20) in α-helix conformation A. (*A*) The hydrophobic face. (*B*) The polar face. The electrostatic potential (ϕ), calculated using DelPhi (Nicholls and Honig, 1991) is color-coded and displayed on the molecular surface using GRASP (Nicholls et al., 1991). Negative potentials (0 kT/e $> \phi >$ −20 kT/e) are red, positive potentials (0 kT/e $< \phi <$ 20 kT/e) are blue, and neutral potentials are white. The peptide is shown with its N-terminus pointing upward.

with the vast majority of the experimental data mentioned above.

It is noteworthy that Efremov et al. used eight analogs of HA2(1–20), some of which are fusogenic and some not, and that the most likely conformations and orientations of all of them were nearly identical to that of the HA2(1–20) peptide (Table 1 of Efremov et al., 1999b). The fact that the depth of penetration into the hydrocarbon region and the tilt angle of all the peptides were so similar, even though most of them involved mutations of five or more residues, suggests that the energy function used in the simulations may be unintentionally biased to favor oblique orientations. The free energy values associated with the lowest free energy states were ~ -200 kcal/mol, which are obviously far too negative for a biological processes. Thus, while Efremov et al. were able to reproduce the experimental data, their study does not further our understanding of the energetics of the interaction of fusion peptides with bilayers.

We present here the results of continuum solvent model calculations of the free energy of association of the HA fusion peptide with lipid bilayers, in order to provide preliminary guidelines toward a fundamental understanding of the energetics of the system.

METHODS

A spontaneous partitioning of a peptide into a membrane requires that its free energy of transfer from bulk water to the membrane be negative. The total free energy of this process is a sum of various contributions (Ben-Tal et al., 1996a; Engelman and Steitz, 1981; Jacobs and White, 1989; Jahnig, 1983; Kessel and Ben-Tal, 2000; Milik and Skolnick, 1993; White and Wimley, 1999):

$$\Delta G_{tot} = \Delta G_{el} + \Delta G_{np} + \Delta G_{imm} + \Delta G_{lip} + \Delta G_{con} \quad (1)$$

Some of these contributions—the electrostatic (ΔG_{el}) and nonpolar (ΔG_{np}) contributions to the solvation free energy—were calculated here using the continuum solvent model (Gilson, 1995; Honig and Nicholls, 1995; Nakamura, 1996; Warshel and Papazyan, 1998). Others, such as molecule immobilization effects (ΔG_{imm}), lipid perturbation effects (ΔG_{lip}), and the free energy of the molecule's conformational changes (ΔG_{con}), were estimated.

Experimental data and theoretical studies in similar systems (Kessel and Ben-Tal, 2000; White and Wimley, 1999) suggest that the major contribution to the total free energy comes from the solvation free energy, defined as:

$$\Delta G_{sol} = \Delta G_{el} + \Delta G_{np}. \quad (2)$$

ΔG_{sol} is the free energy of transfer of a peptide from water into the lipid phase of the membrane. It accounts both for electrostatic contributions (ΔG_{el}) resulting from changes in the solvent dielectric constant and for van der Waals and solvent structure effects, which are grouped in the nonpolar term (ΔG_{np}) and together define the classic hydrophobic effect. We calculated ΔG_{sol} using the continuum solvent model. The method has been described in detail in earlier studies of the membrane association of polyalanine α-helices (Ben-Tal et al., 1996a) and the antimicrobial peptide, alamethicin (Kessel et al., 2000a; reviewed by Kessel and Ben-Tal, 2000). Here we present a brief outline, with emphasis on the minor changes that were made to adapt the method to the HA fusion peptide.

Electrostatic contributions

The electrostatic contributions, ΔG_{el}, can be obtained from finite difference solutions to the Poisson-Boltzmann equation (the FDPB method) (Honig and Nicholls, 1995; Honig et al., 1993). We calculated the electrostatic free energy by integration over the potential, multiplied by the charge distribution in space. The peptides were represented in atomic detail, with atomic radii and partial charges defined at the coordinates of each nucleus. The charges and radii were taken from PARSE, a parameter set that was derived to reproduce vacuum-to-water (Sitkoff et al., 1994) and alkane-to-water (Sitkoff et al., 1996) solvation free energies of small organic molecules. It has been successfully used in the study of many biological systems, such as polyalanine α-helix insertion into lipid bilayers (Ben-Tal et al., 1996a), formation of amide hydrogen bonds (Ben-Tal et al., 1997), the membrane permeability of monensin-cation complexes (Ben-Tal et al., 2000b), alamethicin insertion into lipid bilayers (Kessel et al., 2000a) and alamethicin flip-flop motion in bilayers (Kessel et al., 2000b).

In the FDPB calculations reported here, the boundary between the peptides and the solvents (water or membrane) was set at the contact surface between the van der Waals surface of the peptide and a solvent probe (defined here as having a 1.4 Å radius; Sharp et al., 1991)). The peptides and the lipid bilayer were assigned a dielectric constant of 2 and water a dielectric constant of 80. The system was mapped onto a lattice of 145^3 grid points, with a resolution of 3 points per Å, and the Poisson equation was numerically solved for the electrostatic potential.

Nonpolar contributions

The nonpolar contributions to the solvation free energy are due mainly to the hydrophobic effect and are assumed to be linearly proportional to the water-accessible surface area of the molecules (Nozaki and Tanford, 1971). The proportionality constant $\gamma = 0.0278$ kcal/(mol · Å^2) (commonly referred to as "surface tension") and an intercept $b = -1.71$ kcal/mol have been derived from the partitioning of alkanes between liquid alkane and water (Sitkoff et al., 1996).

Peptide structure

We used the peptide GLFGAIAGFIENGWEGMIDG, which corresponds to HA2(1–20) of the X:31 strain. In view of the available experimental evidence, the peptide was built as a canonical right-handed α-helix, using Insight97/Biopolymer (MSI, San Diego, CA). Two helices that differed in the rotameric state of Phe-3 were built for reasons that are explained in the Results below. The first was built with the optimum combination of rotamers, which produces the lowest internal energy, as found by the automatic procedure of Insight97/Biopolymer/AutoRotamer. The structure was energy-minimized using the 100 steepest descent iterations and the CVFF force field in DISCOVER. We refer to this helix as helix A. To create the second model α-helix, referred to here as helix B, the rotamer of Phe-3 was changed using Insight97/Biopolymer/manual Rotamer to optimize ΔG_{sol} as explained the Results below.

The electrostatic potential map calculated for the helices illustrates their amphipathic nature and suggests that they may be adsorbed horizontally on membrane surfaces. In such orientation the residues in the hydrophobic face (Fig. 1 *A*) may interact favorably with the lipid chains of the membrane, while residues in the polar face (Fig. 1 *B*) may interact with the polar headgroups and the water. The alternative, i.e., a vertical insertion of the helices into the membrane, is unlikely because it would involve the high free energy penalty of membrane insertion of the polar residues shown in Fig. 1 *B*.

Membrane structure

Lipid membranes are fluid and it is therefore impossible to determine their high-resolution 3D structures. This is one of the main difficulties in

investigating membrane proteins using computational tools. However, diffraction methods have provided a wealth of structural information about the distribution of the different chemical groups of the lipids and water molecules across the bilayer (White and Wimley, 1999). We therefore represented the membrane as a slab of 30 Å in width with a dielectric constant of 2, based on a combination of thickness and capacitance measurements (Dilger and Benz, 1985; Fettiplace et al., 1971). This is a very simple model that does not present the structure of the hydrocarbon chains and the phosphate headgroups. However, despite its limitations, the model accurately takes into account desolvation effects, which are often the dominant contributions to the free energy of association of peptides with unperturbed lipid membranes (Ben-Tal et al., 1996a, 2000b; Kessel et al., 2000a).

Lipid perturbation

ΔG_{lip} is the free energy penalty resulting from the interference of the solute (the peptide) with the conformational freedom of the lipid bilayer chains. $\Delta G_{lip} = 2.3$ kcal/mol has been calculated for the vertical insertion of a polyalanine α-helix into the lipid bilayer (Ben-Shaul et al., 1996; Ben-Tal et al., 1996a). Our results showed that a minimum in ΔG_{sol} appears for horizontal association of the α-helix. In such cases there is very little contact between the peptide and the lipid chains, unless the membrane structure is severely disrupted; we thus assumed that $\Delta G_{lip} = 0$. This assumption has also been successfully used previously (Ben-Tal et al., 1996a; Kessel et al., 2000a, b).

It should be noted that our model does not consider the possible effects of local membrane deformation on ΔG_{sol} and ΔG_{lip}. That is, if peptide-membrane association involves the transfer of a polar group into the hydrocarbon region of the bilayer, the membrane may undergo a local deformation to reduce the desolvation free energy penalty due to this process. This local deformation may involve a ΔG_{lip} penalty, the magnitude of which is usually small compared to the electrostatic desolvation free energy penalty (Ben-Shaul et al., 1996). This issue will be considered below.

Peptide immobilization

ΔG_{imm} is the free energy penalty resulting from the confinement of the external rotational and translational motions of the peptide inside the membrane. An upper bound value of $\Delta G_{imm} = 3.7$ kcal/mol has been calculated for the vertical insertion of soluble polyalanine α-helices into the lipid bilayer (Ben-Shaul et al., 1996; Ben-Tal et al., 1996a). Very recently, we estimated a value of $\Delta G_{imm} = 1.3$ kcal/mol based on continuum solvent model calculations of the electrostatic adsorption of pentalysine onto membranes containing acidic lipids (Ben-Tal et al., 2000a). In the present study, we used the value derived from the peptalysine-membrane system because both the fusion peptide and pentalysine are adsorbed on the membrane surface.

Peptide conformational changes

ΔG_{con} is the free energy involved in the conformational changes of the peptide between the two phases. Experimental studies have indicated that the conformation of synthetic peptides corresponding to the HA's fusion peptide varies during transfer from water to lipid bilayers. Early CD experiments indicated that the peptides are random coils in the aqueous phase, but adopt a helical conformation in the membrane (Lear and DeGrado, 1987); later studies showed an organized α/β structure in water that either transforms into a helical structure (Luneberg et al., 1995) or remains in an α/β structure (Gray et al., 1996). The stability of polyalanine α-helices has been the subject of theoretical (Yang and Honig, 1995) and experimental (e.g., Altmann et al., 1990) studies. These studies indicate that a complete helix-to-coil transition of a polyalanine helix of ~10 residues involves a free energy value close to zero. Because we do not know for certain the secondary structures of the fusion peptide in the aqueous phase and in the membrane, it is difficult to estimate ΔG_{con}. The experimental data suggest that the insertion into the membrane involves a transformation from one organized structure to another, and we therefore assumed that ΔG_{con} is insignificant and could be neglected.

RESULTS

The available experimental data suggest that the HA fusion peptide associates with lipid membranes in α-helical conformation and in a surface rather than transmembrane orientation. We therefore calculated the free energy of interaction of the two helices, A and B, in surface orientations, with respect to our model of the membrane, as described in the Methods. The electrostatic maps of Fig. 1, *A* and *B* and the experimental data mentioned above indicate that the peptide is oriented with its hydrophobic face (Fig. 1 *A*) toward the membrane and its polar face (Fig. 1 *B*) immersed in water, away from the membrane. We therefore started with this horizontal orientation (Fig. 2 *A*) and used it as a reference throughout the paper.

In Fig. 2 *B*, the electrostatic, nonpolar, and solvation contributions to the free energy of interaction of the HA2(1–20) peptide with the membrane are presented as a function of the distance, *h*, between the geometrical center of the helix and the membrane midplane. The peptide is oriented horizontally to the membrane as depicted in Fig. 2 *A*. The hydrophobic face of the helical peptide is just in contact with the membrane at $h = 21$ Å, while at $h = 0$ (not shown), the principle axis of the helix coincides with the membrane midplane. ΔG_{np}, the driving force for insertion, increases in size along the insertion process. Likewise, the electrostatic penalty for insertion increases along the insertion process because more polar groups are inserted into the membrane. However, because of the hydrophobic nature of the helix face that is in direct contact with the membrane, the electrostatic interactions only become significant at $h = 17$ Å, when the polar groups of the peptide backbone are in contact with the bilayer.

The sharp increase in ΔG_{el} practically prevents the helix from crossing the membrane in the horizontal orientation of Fig. 2 *A*; the helix therefore resides in the configuration associated with the minimum in the solvation free energy curve obtained at $h = 17$ Å. In this configuration, the helical fusion peptide is adsorbed at the water-bilayer interface, with its hydrophobic face dissolved in the bilayer and its hydrophilic face in the water. The solvation free energy value at the minimum is the sum of the nonpolar interactions that are the driving force of the insertion process (~−16 kcal/mol) and the electrostatic penalty (~7 kcal/mol), that is, $\Delta G_{sol} \approx -9$ kcal/mol.

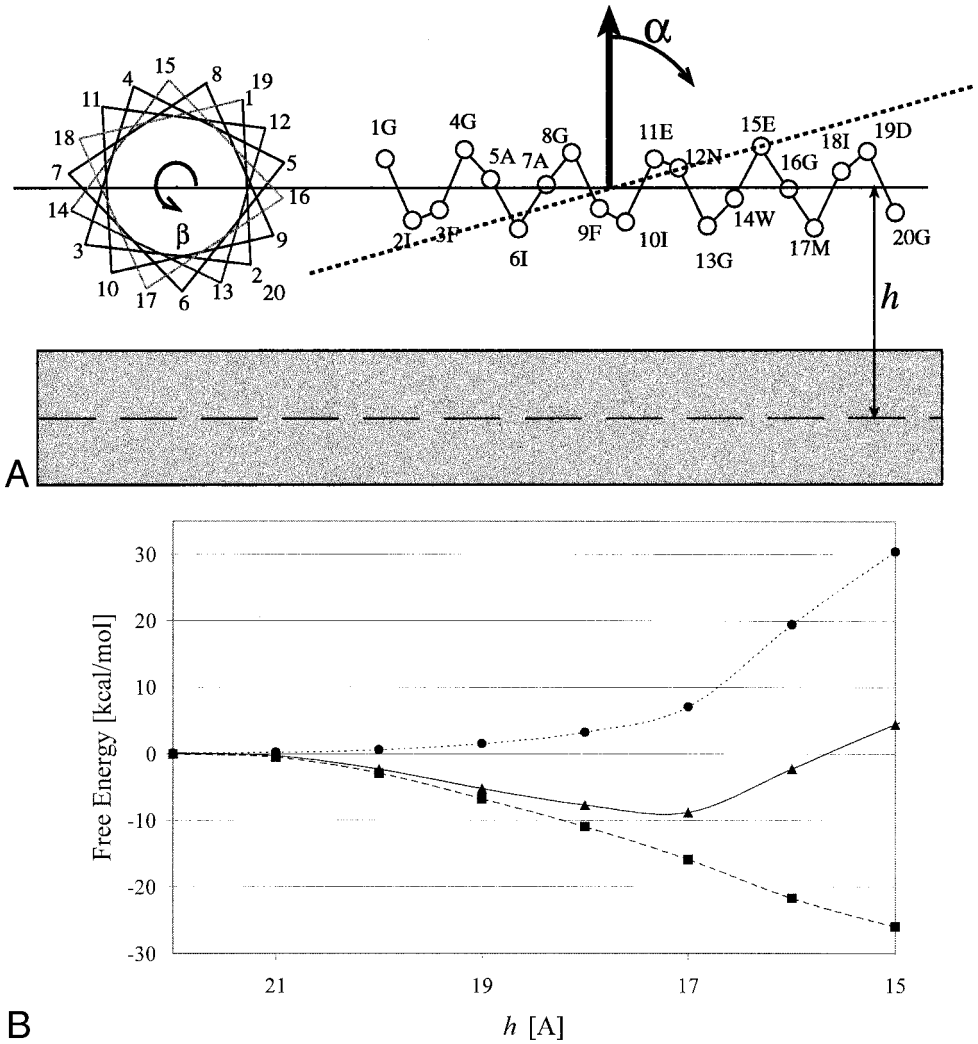

FIGURE 2 (*A*) A schematic diagram showing a hypothetical insertion process of the HA2(1–20) fusion peptide into the lipid bilayer in a horizontal orientation, in which the principal axis of the peptide is parallel to the membrane surface. HA2(1–20), in the experimentally observed amphipathic α-helical structure (conformation A), is depicted as a helical wheel on the left-hand side and in trace representation on the right-hand side. The hydrophobic core of the lipid bilayer, represented in the model as a slab of dielectric constant $\epsilon = 2$, is depicted by the gray rectangle. The white surroundings represent the water, with a dielectric constant $\epsilon = 80$. The distance h, between the geometrical center of HA2(1–20) and the midplane of the lipid bilayer, and the rotational angles α and β are indicated. (*B*) Insertion of HA2(1–20) in α-helix conformation A and the orientation of Fig. 2 *A* into a lipid bilayer. The electrostatic (●), nonpolar (■), and solvation (▲) free energies of the peptide-membrane system are plotted as functions of h. The zero of the free energy for the helix was chosen as $h = \infty$. The membrane width is 30 Å, and the model of the peptide was built as described in the Methods. The calculations were carried out on a lattice of 145^3 points and a resolution of 3 grid points/Å.

The calculated most favorable peptide-membrane configurations

We carried out a comprehensive search over a large number of orientations of HA2(1–20) in the conformation of helix A at distances of h = 15–25 Å from our model of the lipid bilayer. In all the orientations that were searched, the ΔG_{np} contributions were around −17 kcal/mol. In contrast, the ΔG_{el} penalties varied between ~2 and 22 kcal/mol, mainly due to insertion of the polar groups of the peptide backbone (both hydrogen-bonded and non-bonded) into the hydrocarbon region of the membrane.

Fig. 3 *A* presents the results that were obtained for peptide-membrane configurations in the vicinity of the ΔG_{sol} minimum obtained at the horizontal orientation (Fig. 2 *B*). The collection of solvation free energy values associated with HA2(1–20) in the conformation of helix A, referred to as the "solvation potential surface," had a basin shape with a minimum at β of between −33° and −4° and at α of between 86° and 90° (approximately the dark blue region in Fig. 3 *A*), when the helix was adsorbed at the membrane-water interface in horizontal orientation. The value of the solvation free energy at the bottom of the basin was ~−8 to −9 kcal/mol.

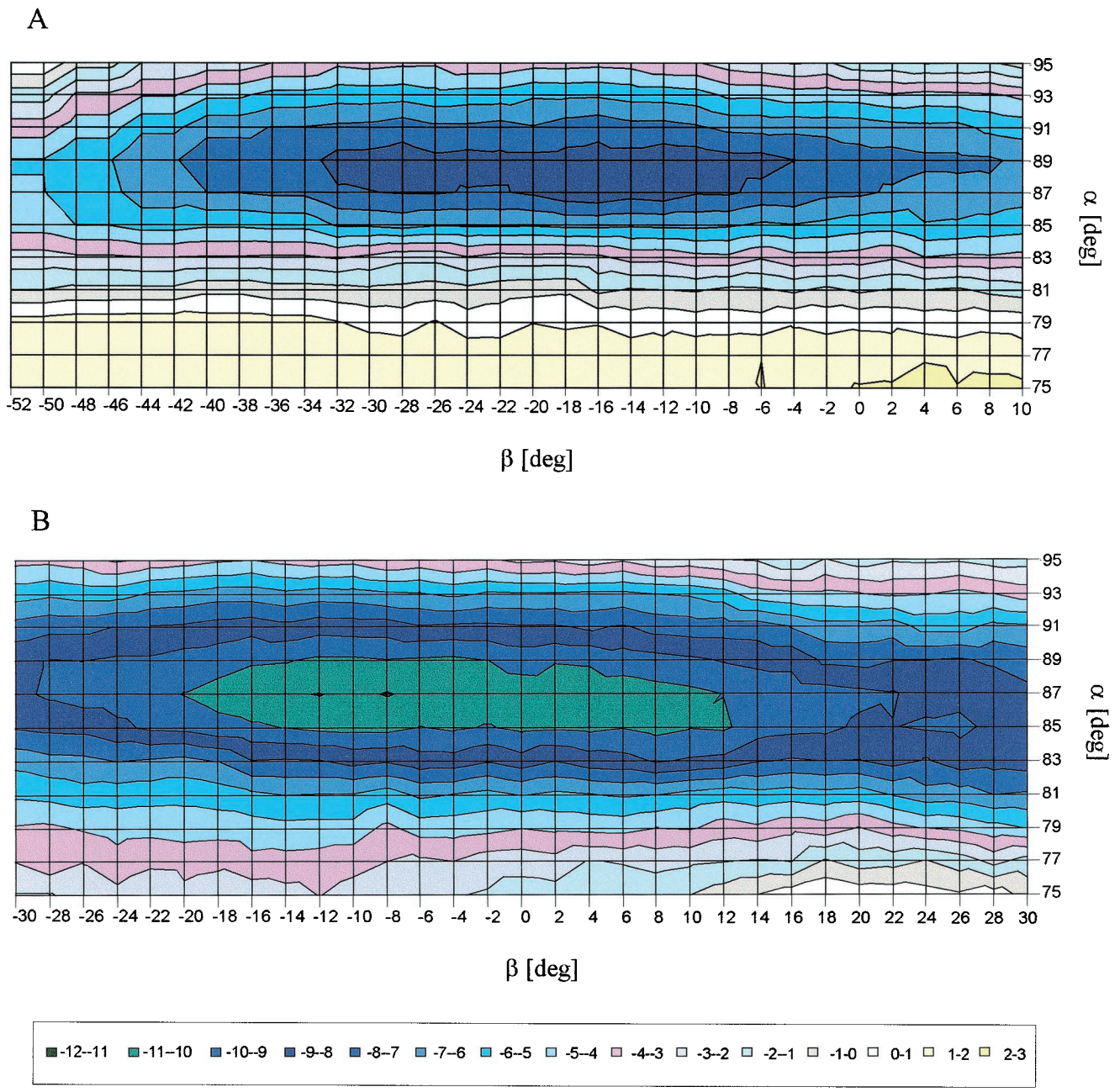

FIGURE 3 ΔG_{sol} of the fusion peptide, in helical conformations A (*A*) and B (*B*), as a function of the rotation angles α and β with respect to the horizontal orientation of Fig. 2 *A*. The distance between the geometrical center of the helix and the membrane midplane is $h = 17$ Å.

Fig. 4 *A* illustrates the position of the HA2(1–20) helix relative to the membrane in one of the most favorable configurations of Fig. 3 *A*. It is evident from the figure that the hydrophobic face of the helix, which is distinctly seen in Fig. 1 *A*, is dissolved in the lipid bilayer while the polar face, which appears in Fig. 1 *B*, is water-exposed. In the most favorable orientations the electrostatic contributions are rather small, indicating that only a few polar atoms are dissolved in the lipid bilayer. The total free energy of transfer of HA2(1–20) from water into the hydrocarbon region of the membrane in the horizontal orientation of Fig. 4 *A* (calculated using Eq. 1) is $\Delta G_{tot} = \Delta G_{el} + \Delta G_{np} + \Delta G_{imm} = 7 - 16 + 1.3 \approx -7.7$ kcal/mol (Table 1).

Effects of rotameric states

It is evident from the calculations described above that the nonpolar contributions are dominant in the system. It therefore seems that the rotamers, especially of the hydrophobic

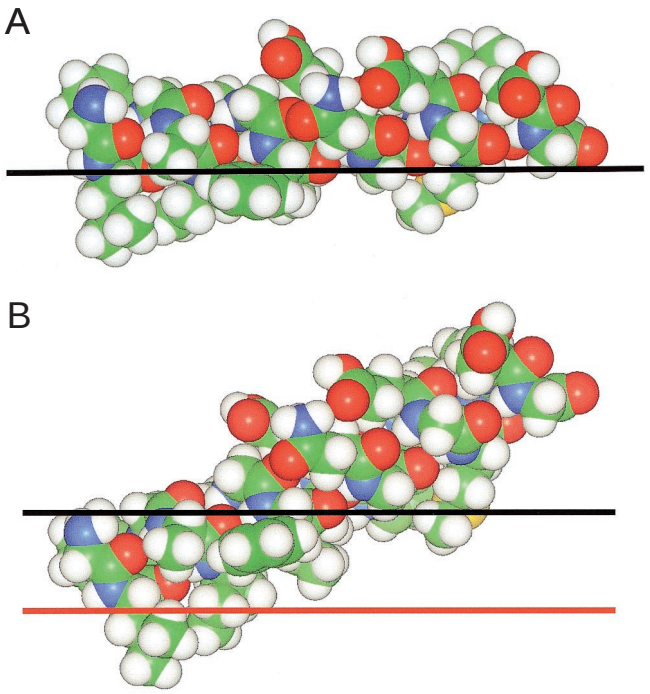

FIGURE 4 A comparison of the theoretically predicted (*A*) and experimentally determined (*B*) orientations of HA2(1–20) (in α-helix conformation A) in the lipid bilayer. The models of the peptide were displayed with INSIGHT (MSI, San Diego, CA). Carbon atoms are green, hydrogen atoms white, oxygen atoms red, and nitrogen atoms blue. The horizontal lines through each model represent the boundary between the water-membrane interface (*above*) and the hydrocarbon region of the lipid bilayer (*below*). (*A*) HA2(1–20) in a horizontal orientation with respect to the lipid bilayer. This orientation ($h \approx 17$ Å, $\alpha \approx 87°$, and $\beta \approx -16°$) is associated with one of the most negative ΔG_{sol} values of Fig. 3 *A*. (*B*) The experimentally observed, oblique orientations of Macosko et al. (1997) and of Zhou et al. (2000). In these two orientations $\alpha \approx 65°$ and $\beta \approx 0°$, but the penetration depths correspond to $h \approx 18$ Å (*black line*) and ≈23 Å (*red line*), respectively.

residues that dissolve in the lipid bilayer, may have a crucial influence on the value of ΔG_{sol}. It is recognizable from the molecular model of the peptide (Fig. 4 *A*) that, due to its rotameric state, the aromatic ring of Phe-3, which could add to the nonpolar free energy, is outside the hydrocarbon region of the membrane. Therefore, we used the rotamer library, as described in Methods, to modify the rotameric state of Phe-3 so that the aromatic ring was closer to the hydrophobic face of the helix. The structure thus obtained is referred to as helix B.

We carried out the same set of calculations with HA2(1–20) in the conformation of helix B and the results are presented in Fig. 3 *B*. The main features of the orientation remain the same. The α-helix is more or less fixed in a nearly parallel orientation with respect to the membrane surface, forming an angle (α) of 85–89° with the normal of the membrane, and is free to rotate around its principal axis (β) in a range of ~32°. Because the aromatic ring of Phe-3 interacts favorably with the lipid bilayer, the value of ΔG_{np} at the minimum increased in size and so did the solvation free energy. Therefore, $\Delta G_{sol} \approx -11$ kcal/mol, as opposed to the value of ≈ -9 kcal/mol obtained for helix A. The most negative solvation free energy value, $\Delta G_{sol} = -12$ kcal/mol, was obtained for two configurations (Fig. 3 *B*, $\alpha = 87°$ and $\beta = -12°$; $\alpha = 87°$, $\beta = -8°$). However, the helix can probably assume any of the configurations that are thermally accessible, i.e., the entire configurational space within ~kT ≅ 0.6 kcal/mol of the most negative solvation free energy (approximately the dark green area in Fig. 3 *B*).

The total free energy of transfer of HA2(1–20) in the conformation of helix B from water into the hydrocarbon region of the membrane is $\Delta G_{tot} = \Delta G_{sol} + \Delta G_{imm} = -11 + 1.3 \approx -9.7$ kcal/mol (Table 1).

The experimentally observed orientations

In contrast to our calculations, the HA fusion peptide is experimentally observed in oblique, rather than horizontal, orientations. For example, Macosko et al. (1997) reported a configuration that corresponds to $h \approx 18$ Å, $\alpha \approx 65°$, and $\beta \approx 0°$ (Fig. 4 *B*, *black line*), and Zhou et al. (2000) reported a configuration corresponding to $h \approx 23$ Å, $\alpha \approx 65°$, and $\beta \approx 0°$ (Fig. 4 *B*, *red line*). Indeed, one can clearly see from the electrostatic map in Fig. 1 *A* that the oblique orientation may allow the peptide to partition into the bilayer with the hydrophobic patch near the N-terminus immersed in the bilayer, while the more polar C-terminus remains at the water-bilayer interface. We calculated the values of ΔG_{sol} of HA2(1–20), in the conformations of helix A and B, in these orientations with respect to the bilayer.

The orientation of Macosko et al. (1997)

The calculated values of ΔG_{sol} of HA2(1–20), in the conformations of helices A and B, in the oblique orientation of Macosko et al. (1997) with respect to the bilayer (Fig. 4 *B*, *black line*) were ≈4.0 kcal/mol and ≈3.0 kcal/mol, respectively (Table 1). These values are ~13–14 kcal/mol more positive than the corresponding values obtained in the horizontal configurations (Fig. 4 *A*). The difference is due to changes both in the electrostatic and nonpolar contributions to ΔG_{sol}. The value of ΔG_{np} associated with the oblique orientation (Fig. 4 *B*) is smaller in magnitude by ~3 kcal/mol compared to that of the horizontal orientation (Fig. 4 *A*), since a smaller area of the peptide is dissolved in the membrane in the oblique orientation. The major free energy difference between the oblique (Fig. 4 *B*, *black line*) and horizontal (Fig. 4 *A*) orientations is ~10–11 kcal/mol; it comes from the ΔG_{el} contribution.

In order to further understand the sources of the difference in ΔG_{el} of the oblique versus horizontal orientations of HA(1–20), we closely examined polar groups of the peptide expected to have undergone different interactions with the hydrocarbon region of the bilayer in the two orientations. To

TABLE 1 Summary of the calculated free energy values obtained for HA2(1–20) in the horizontal orientation, which was found here to be the most likely orientations of the peptide in the bilayer, and in two of the experimentally observed oblique orientations

Orientation and Conformation	h* (Å)	α† (°)	β‡ (°)	ΔG_{el}§ (kcal/mol)	ΔG_{np}¶ (kcal/mol)	ΔG_{sol}‖ (kcal/mol)	ΔG_{imm}** (kcal/mol)	ΔG_{tot}†† (kcal/mol)
Horizontal								
A	17	87	−16	7.0	−16.0	−9.0	1.3	−7.7
B	17	87	−8	8.0	−19.0	−11.0	1.3	−9.7
Oblique (Macosko et al., 1997)								
A	18	65	0	17.0	−13.0	4.0	1.3	5.3
B	18	65	0	19.7	−16.7	3.0	1.3	4.3
Oblique (Zhou et al., 2000)								
A	23	65	17	1.7	−2.4	−0.7	1.3	0.6
B	22	65	17	2.1	−5.9	−3.8	1.3	−2.5

"A" and "B" mark the helix conformation used in the calculations.
*Distance h between the geometrical center of the helix and the membrane midplane.
†Rotational angle α.
‡Rotational angle β.
§Electrostatic free energy.
¶Nonpolar free energy.
‖Solvation free energy.
**Immobilization free energy.
††Total free energy.

this end, we neutralized one group at a time by arbitrarily setting its partial atomic charges to zero. Our results show that the ~10 kcal/mol difference in ΔG_{el} is predominantly due to the penalty associated with the transfer of the backbone amide groups at positions 1, 2, 3, and 4 of HA2(1–20). These unsatisfied hydrogen-bonding groups remain at the polar phase in the horizontal orientation of Fig. 4 *A*, while they are buried in the hydrocarbon region of the bilayer in the oblique orientation of Fig. 4 *B* (*black line*).

The orientation of Zhou et al. (2000)

The calculated values of ΔG_{sol} of HA2(1–20), in the conformations of helices A and B, in the oblique orientation of Zhou et al. (2000) with respect to the bilayer (Fig. 4 *B*, *red line*) were ≈ -0.8 kcal/mol and ≈ -3.8 kcal/mol, respectively (Table 1). [Because the depth of the insertion of the helix was not well defined by Zhou et al., the h values were obtained from a minimization along h and correspond to $h \approx 23$ Å and $h \approx 22$ Å, respectively.] These values are ~8 kcal/mol less negative than the corresponding values obtained for the horizontal configuration of Fig. 4 *A*. In the Zhou et al. (2000) orientation, the peptide barely touches the hydrocarbon region of the bilayer. Thus, both the nonpolar and electrostatic contributions to ΔG_{sol} are small in size. The value of ΔG_{np} associated with the oblique orientation (Fig. 4 *B*, *red line*) is smaller in magnitude by ~13 kcal/mol compared to that of the horizontal orientation of Fig. 4 *A*, as a much smaller area of the peptide is dissolved in the membrane in the oblique orientation. The rest of the free energy difference between the oblique and horizontal orientations (Fig. 4 *B*, *red line*, and Fig. 4 *A*), ~5 kcal/mol, comes from the ΔG_{el} contribution.

Convergence tests

We repeated the calculations of Fig. 2 *B* using different grid sizes (145^3 and 193^3) and scales (3 and 4 grid points/Å) to test the convergence of the calculations. The results, presented in Table 2, showed that the calculations of the electrostatic and the nonpolar contributions converge to <0.2 kcal/mol. The values of the solvation free energy converge to <0.04 kcal/mol. The high precision of the solvation free energy calculations results from the opposite changes in ΔG_{np} and ΔG_{el}, which compensate for each other. It may be possible to encounter a case where the nonpolar and electrostatic contributions are added to each other. Under such circumstances, the values of the solvation free energy would converge to <0.4 kcal/mol, which is still

TABLE 2 Results of a series of calculations to test the convergence of the continuum solvent model calculations for HA2(1–20) in the lipid bilayer

Grid Size (grid points)	Scale (grids/Å)	ΔG_{el}* (kcal/mol)	ΔG_{np}† (kcal/mol)	ΔG_{sol}‡ (kcal/mol)
145^3	3	7.069	−15.887	−8.819
193^3	3	7.074	−15.887	−8.813
193^3	4	7.234	−16.091	−8.857

Calculations were carried out using helix A in the horizontal orientation of Fig. 4 *A*.
*Electrostatic free energy.
†Nonpolar free energy.
‡Solvation free energy.

sufficient for this study. Notice, however, that the high precision of our calculations is due to the simplified model we used. The approximated structure used for HA2(1–20) and the representation of the hydrocarbon region of the membrane as a structureless slab of low dielectric constant may result in an error that is difficult to estimate for this system, but which may be much larger than 0.4 kcal/mol, as discussed in detail below.

DISCUSSION

In this research, the free energy of membrane association of the HA2(1–20) fusion peptide was calculated to find the most favorable configurations of the peptide-membrane system. Based on the spectroscopic measurements described in the Introduction, we modeled the peptide as a canonic α-helix. Our results show that the α-helix can associate with the membrane and that its theoretically most favorable orientations are when it is adsorbed horizontally on the surface of the bilayer. Such orientations were recently found for the amphipathic α-helices in the x-ray crystal structures of the membrane exposed face of the peripheral membrane proteins Cox1 and Cox2 (Kurumbail et al., 1996; Picot et al., 1994). They are also in accord with various measurements (Han et al., 1999; Luneberg et al., 1995; Macosko et al., 1997) in which spectroscopic techniques were used to determine the orientation of the HA fusion peptide in membranes. However, although our calculations suggest approximately horizontal orientations (Fig. 4 *A*), the experimental data on the HA fusion peptide indicate oblique orientations (Fig. 4 *B*). This issue is discussed further below, but we will first consider recent Monte Carlo simulations of the HA2(1–20) fusion peptide (Efremov et al., 1999b).

These simulations were based on a Monte Carlo search over the conformational and configurational space of HA2(1–20), which was described in atomic detail, in association with membranes that were described using a slab model. The simulations support the general view that the peptide is likely to assume an α-helical structure in an oblique orientation with an angle of $\sim$15° from the membrane plane. In the most likely configurations obtained in these simulations, the N-terminus of the peptide was buried inside the hydrophobic core of the membrane. In contrast to our calculations, the results of these simulations are in very close agreement with the vast majority of the available experimental evidence (but see Zhou et al. (2000)).

The results of the two sets of calculations are highly dependent on the methodology used for estimating the solvation free energy. Thus, it is very important that the solvation parameters are reliable. We used the continuum solvent models described by Ben-Tal et al. (1996a) and Kessel et al. (2000a), and the PARSE set of atomic charges and radii of Sitkoff et al. (1996) that was carefully tested and successfully reproduced experimental data both for small molecules and for peptides. Efremov et al.'s methodology (1999a) involved deriving a set of atomic solvation parameters. The performance of the solvation parameters is inferior to the continuum solvent method, as indicated by comparing the success of these two methods in reproducing experimental values of the solvation free energy of small molecules (Sitkoff et al., 1994, Fig. 5, and Sitkoff et al., 1996, Fig. 4 vs. Efremov et al., 1999a, Fig. 2, *B* and *C*).

In general, continuum solvent models are expected to be superior to methods that are based on atomic solvation parameters, because in continuum solvent models local environmental effects on each atom are taken explicitly into account. For example, while an oxygen atom in a carboxyl group is given the same solvation parameter regardless of whether it is involved in a hydrogen bond, in continuum solvent models the presence or absence of hydrogen bonds is explicitly taken into account. Thus, one would expect that the performance of Efremov et al.'s model for larger molecules, for example peptides, would be much worse than for small molecules. Indeed, Efremov et al. (1999a) reported a solvation free energy value of ~ -30 kcal/mol for the transfer of a 25-mer polyalanine α-helix from the aqueous phase into the bilayer, while continuum solvent model calculations provide a value of ~ -4 kcal/mol (Ben-Tal et al., 1996a), in close agreement with the experimental value of ~ -5 kcal/mol (Moll and Thompson, 1994).

Overall, it appears that the method of Efremov et al. tends to produce overly negative solvation free energy values. This may explain the unrealistic free energy values (of ~ -200 kcal/mol) reported by Efremov et al. for the transfer of the HA2(1–20) fusion peptide and analogs from the aqueous phase into the bilayer (1999b). Hence, the agreement between these calculations and the experimental data mentioned above, regarding the most likely orientation of the fusion peptide in lipid bilayers, may be fortuitous.

We now return to the calculations reported here and outline some of the model's limitations. The disparity between the experimental data and the calculations may be due to each, or to all, of these limitations.

A major uncertainty in the model results from the absence of a high-resolution structure of the fusion peptide. The experimental data are based on spectroscopic methods that can provide only partial information about the secondary structure of the peptide at low resolution. The vast majority of experimental data supports a helical structure (Brasseur et al., 1990; Lear and DeGrado, 1987; Luneberg et al., 1995; Macosko et al., 1997; Takahashi, 1990; Zhou et al., 2000; but see Gray et al., 1996). The lack of accurate structural information forced us to use the computer-designed model of the peptide of Fig. 2 *A*. The secondary structure was assumed to be a canonical α-helix, but because there are a variety of residues of different sizes that have different polar groups, it is obvious that an accurate 3D structure would have a crucial effect on the results. A comparison of the results of Fig. 3 *A* to Fig. 3 *B*, which differ from each other in the rotameric state of a single residue (Phe-3), provides

an example of how sensitive the results can be to structural changes in the peptide. The results presented in these figures are qualitatively the same in that both indicate that HA2(1–20) is most likely to associate with the bilayer in horizontal orientations. The ΔG_{sol} value associated with this orientation differs by ~2 kcal/mol, depending on the rotameric state of Phe-3 (Table 1).

The description of the lipid bilayer as a slab of low dielectric constant obscures all atomic detail about peptide-bilayer interactions. However, as discussed elsewhere (Ben-Tal et al., 1996a, 2000b; Berneche et al., 1998; Biggin et al., 1997; Kessel et al., 2000a), the slab model is a standard representation of the hydrocarbon region of lipid bilayers. This depiction is likely to provide a reasonable model for bilayer effects on electrostatic interactions so long as the bilayer is not significantly perturbed by the peptide.

The calculated solvation free energy value depends strongly on the value assigned to the inner dielectric constant and on the choice of the set of atomic partial charges and radii. However, PARSE yields accurate transfer free energies between water and liquid alkane for small organic molecules containing the amino acid backbone and side chains (Sitkoff et al., 1996). It therefore seems reasonable to assume that it provides a good approximation for the water-membrane solvation properties of peptides (such as the HA fusion peptide) that are constructed from the same chemical groups. Moreover, the nonpolar surface tension coefficient used in PARSE, which is deduced from the partitioning of nonpolar molecules between water and liquid alkane, is nearly identical to that recently reported for the transfer of nonpolar molecules into lipid bilayers (Buser et al., 1994; Thorgeirsson et al., 1996). Finally, the success of the model in reproducing experimental data on the membrane-association of peptides and ionophores indicates its strength in cases where solvation effects dominate the energetics (e.g., Ben-Tal et al., 1996a, 2000b; Kessel et al., 2000a).

The greatest shortcoming of the model is its complete neglect of the polar headgroup region, which is the site of the fusion peptide adsorption onto the bilayer. This shortcoming may affect the quality of the calculations in three different ways. First, the model assumes a sharp boundary between the dielectric constant of the hydrocarbon region ($\epsilon = 2$) and of the aqueous phase ($\epsilon = 80$). Because the dielectric constant in the headgroup region is estimated to be between 25 and 40 (Ashcroft et al., 1981), this region might most appropriately be regarded as part of the aqueous phase defined in this study. Second, the model fails to account for the physical presence of the polar headgroups; self-avoidance effects due to the van der Waals repulsion between the headgroups and the peptide are therefore missing in the model. The assumption is that the polar headgroups "make room" to accommodate the peptide at the membrane surface. Third, specific interactions between the polar headgroups and chemical groups of the backbone and side chains of the peptide are missing from the model. This may be a serious shortcoming, because the amino acid conservation in the fusion peptide and the sensitivity of the peptide to moderate mutations may be an indication of the importance of such specific interactions (e.g., Han et al., 1999; reviewed by Durell et al., 1997). This issue is considered further below.

Although the model does consider the perturbing effect of the peptide on the structure of the membrane, ΔG_{lip}, it does not consider the possibility that the membrane structure is severely damaged due to the interaction with the peptide. If the structure of the membrane is locally deformed, as suggested by studies by Colotto and Epand (1997) and by Siegel and Epand (2000), and the membrane cannot be described as a slab, the model may even fail to correctly account for the solvation free energy changes due to peptide-membrane interactions. Given its role in membrane fusion, the fusion peptide is expected to destabilize and maybe to deform lipid bilayers, which puts a serious limitation on the utility of the slab model for studying fusion peptide interactions with membranes. This matter is considered further below.

Overall, the results of this study are in accord with the available experimental data (Han et al., 1999; Luneberg et al., 1995; Macosko et al., 1997) but there is disagreement about the details. Both the experimental and theoretical studies indicate that the helix is very unlikely to penetrate the membrane, but is instead located in the interface between the hydrocarbon region of the membrane and the aqueous phase. However, there is a certain discrepancy between the measurements and calculations regarding the exact configuration of the peptide-membrane system. Experimental measurements indicate that the peptide is in an oblique orientation, forming an angle of between 25° and 45° with the membrane plane, and there is conflicting evidence on whether its N-terminal residues are immersed in the hydrocarbon or interface regions of the membrane. In contrast, our calculations suggest that such a configuration is very unlikely in unperturbed lipid bilayers, and that the most favorable configuration of the peptide is with its principle axis essentially parallel to the membrane surface so that both the N- and C-terminal residues are in the aqueous phase.

Of the four experimental studies, Macosko et al. (1997) and Zhou et al. (2000) reported the most detailed structural information. These results enabled a direct comparison of the experimentally determined configurations to the most likely configuration obtained in our calculations (Fig. 4 *A*). The most significant difference between our calculations and the measurements of Macosko et al. (1997) (Fig. 4 *B*, *black line*) is with respect to the N-terminus, which is partially inserted into the hydrocarbon region of the lipid bilayer in the experimentally deduced configuration, but not in the most favorable configuration suggested in our model. The fact that insertion of helix termini into unperturbed bilayers involves a high free energy penalty, and is therefore

very unlikely, has been recognized in the past (Ben-Tal et al., 1996b, 1997; Kessel et al., 2000a) reviewed by Kessel and Ben-Tal (2000) and White and Wimley (1999). The high free energy penalty results from the fact that backbone N-H groups, which are not involved in hydrogen bonds, at the helix terminus, are exposed to the hydrocarbon region of the bilayer. This penalty may be reduced by capping from other residues, i.e., if hydrogen bond acceptors from other residues form hydrogen bonds with these amine groups. However, such a possibility is very unlikely for the fusion peptide, since the nearest hydrogen bond acceptor (the carboxyl group of the Glu-11 side chain) is located ~15 Å away from the N-terminus.

Indeed, the very recent NMR measurements of Zhou et al. (2000) indicate that the N-terminus of HA(1–20) remains protonated and resides close to the aqueous phase. However, our calculations suggest that while such an orientation involves a very small electrostatic free energy penalty, it also involves very small favorable nonpolar contributions to the solvation free energy. Thus, even this configuration appears, in theory, to be only marginally stable.

The most likely explanation for the discrepancy between experimental measurements and our calculations is that the structure of the membrane is severely perturbed due to interaction with the peptide, so that the model overestimates the desolvation free energy penalty of the process, and/or that specific interactions between the polar headgroups and the peptide, missing in the model, overcompensate for the desolvation free energy penalty. The fact that specific interactions between the HA2(1–20) fusion peptide and membrane lipids are important for its fusogenic and membranolytic activities has been reported in the past (Chernomordik et al., 1997; Clague et al., 1993), but this issue clearly needs to be studied further. Another possibility is that the discrepancy between experimental measurements and the calculations results from our use of a sharp and non-physical dielectric boundary between the membrane and the aqueous phase in the calculations.

In conclusion, although the calculations reported here are not in full agreement with the experimental data regarding the most favorable orientation of the HA2(1–20) fusion peptide in lipid bilayers, they provide a reasonable value of the free energy of peptide-membrane association, as well as a breakdown into the different free energy components. They also seem to indicate the presence of yet another intermediate state in HA-mediated membrane fusion (Fig. 4 *A*). The state is characterized by the horizontal adsorption of HA2(1–20) onto the surface of an unperturbed lipid bilayer. This state is significantly stable: ~8–10 kcal/mol more stable than HA2(1–20) in solution. However, because the model that we used is highly approximated and this state was not detected experimentally, its existence is questionable. The calculations suggest that the experimentally observed oblique orientation of Macosko et al. (1997) involves a large desolvation free energy penalty, mainly due to the transfer of backbone N-H groups at the N-terminus of the peptide from the aqueous phase, and that this orientation is therefore very unlikely. This penalty is avoided in the recently observed orientation of Zhou et al. (2000), but even this orientation appears to be significantly less stable than the horizontal one. How the desolvation free energy difference (of ~8–14 kcal/mol) between the horizontal and oblique orientations is compensated for, remains to be determined.

We are thankful to Roman Efremov and Richard Epand for their comments on the manuscript.

This work was supported by Israel Science Foundation Grant 683/97-1 and fellowships from the Wolfson and Alon Foundations (to N.B-T.).

REFERENCES

Altmann, K. H., J. Wojcik, M. Vasquez, and H. A. Scheraga. 1990. Helix-coil stability constants for the naturally occurring amino acids in water. XXIII. Proline parameters from random poly(hydroxybutylglutamine-*co*-L-proline). *Biopolymers.* 30:107–120.

Ashcroft, R. G., H. G. Coster, and J. R. Smith. 1981. The molecular organisation of bimolecular lipid membranes. The dielectric structure of the hydrophilic/hydrophobic interface. *Biochim. Biophys. Acta.* 643: 191–204.

Ben-Shaul, A., N. Ben-Tal, and B. Honig. 1996. Statistical thermodynamic analysis of peptide and protein insertion into lipid membranes. *Biophys. J.* 71:130–137.

Ben-Tal, N., A. Ben-Shaul, A. Nicholls, and B. Honig. 1996a. Free-energy determinants of alpha-helix insertion into lipid bilayers. *Biophys. J.* 70:1803–1812.

Ben-Tal, N., B. Honig, C. K. Bagdassarian, and A. Ben-Shaul. 2000a. Association entropy in adsorption processes. *Biophys. J.* 79:1180–1187.

Ben-Tal, N., B. Honig, C. Miller, and S. McLaughlin. 1997. Electrostatic binding of proteins to membranes. Theoretical predictions and experimental results with charybdotoxin and phospholipid vesicles. *Biophys. J.* 73:1717–1727.

Ben-Tal, N., B. Honig, R. M. Peitzsch, G. Denisov, and S. McLaughlin. 1996b. Binding of small basic peptides to membranes containing acidic lipids: theoretical models and experimental results. *Biophys. J.* 71: 561–575.

Ben-Tal, N., D. Sitkoff, S. Bransburg-Zabary, E. Nachliel, and M. Gutman. 2000b. Theoretical calculations of the permeability of monensin-cation complexes in model bio-membranes. *Biochim. Biophys. Acta.* 1466: 221–233.

Bentz, J. 1993. Viral Fusion Mechanisms. CRC Press, Boca Raton, FL.

Bentz, J., H. Ellens, and D. Alfrod. 1993. Architecture of the influenza hemagglutinin membrane fusion site. *In* Viral Fusion Mechanisms. J. Bentz, editor. CRC Press, Boca Raton, FL. 163–200.

Berneche, S., M. Nina, and B. Roux. 1998. Molecular dynamics simulation of melittin in a dimyristoylphosphatidylcholine bilayer membrane. *Biophys. J.* 75:1603–1618.

Biggin, P. C., J. Breed, H. S. Son, and M. S. Sansom. 1997. Simulation studies of alamethicin-bilayer interactions. *Biophys. J.* 72:627–636.

Brasseur, R., M. Vandenbranden, B. Cornet, A. Burny, and J. M. Ruysschaert. 1990. Orientation into the lipid bilayer of an asymmetric amphipathic helical peptide located at the N-terminus of viral fusion proteins. *Biochim. Biophys. Acta.* 1029:267–273.

Bullough, P. A., F. M. Hughson, J. J. Skehel, and D. C. Wiley. 1994. Structure of influenza haemagglutinin at the pH of membrane fusion. *Nature.* 371:37–43.

Buser, C. A., C. T. Sigal, M. D. Resh, and S. McLaughlin. 1994. Membrane binding of myristylated peptides corresponding to the NH2 terminus of Src. *Biochemistry.* 33:13093–13101.

Carr, C. M., and P. S. Kim. 1993. A spring-loaded mechanism for the conformational change of influenza hemagglutinin. *Cell.* 73:823–832.

Carr, C. M., and P. S. Kim. 1994. Flu virus invasion: halfway there. *Science.* 266:234–236.

Chen, J., K. H. Lee, D. A. Steinhauer, D. J. Stevens, J. J. Skehel, and D. C. Wiley. 1998. Structure of the hemagglutinin precursor cleavage site, a determinant of influenza pathogenicity and the origin of the labile conformation. *Cell.* 95:409–417.

Chernomordik, L. V., E. Leikina, V. Frolov, P. Bronk, and J. Zimmerberg. 1997. An early stage of membrane fusion mediated by the low pH conformation of influenza hemagglutinin depends upon membrane lipids. *J. Cell Biol.* 136:81–93.

Clague, M. J., C. Schoch, and R. Blumenthal. 1993. Toward a dissection of the influenza hemagglutinin-mediated membrane fusion pathway. *In* Viral Fusion Mechanisms. J. Bentz, editor. CRC Press, Boca Raton, FL. 113–132.

Colotto, A., and R. M. Epand. 1997. Structural study of the relationship between the rate of membrane fusion and the ability of the fusion peptide of influenza virus to perturb bilayers. *Biochemistry.* 36:7644–7651.

Dilger, J. P., and R. Benz. 1985. Optical and electrical properties of thin monoolein lipid bilayers. *J. Membr. Biol.* 85:181–189.

Durell, S. R., I. Martin, J. M. Ruysschaert, Y. Shai, and R. Blumenthal. 1997. What studies of fusion peptides tell us about viral envelope glycoprotein-mediated membrane fusions. *Mol. Membr. Biol.* 14: 97–112.

Efremov, R. G., D. E. Nolde, G. Vergoten, and A. S. Arseniev. 1999a. A solvent model for simulations of peptides in bilayers. I. Membrane-promoting alpha-helix formation. *Biophys. J.* 76:2448–2459.

Efremov, R. G., D. E. Nolde, P. E. Volynsky, A. A. Chernyavsky, P. V. Dubovskii, and A. S. Arseniev. 1999b. Factors important for fusogenic activity of peptides: molecular modeling study of analogs of fusion peptide of influenza virus hemagglutinin. *FEBS Lett.* 462:205–210.

Engelman, D. M., and T. A. Steitz. 1981. The spontaneous insertion of proteins into and across membranes: the helical hairpin hypothesis. *Cell.* 23:411–422.

Fettiplace, R., D. M. Andrews, and D. A. Haydon. 1971. The thickness composition and structure of some lipid bilayers and natural membranes. *J. Membr. Biol.* 5:277–296.

Gething, M. J., R. W. Doms, D. York, and J. White. 1986. Studies on the mechanism of membrane fusion: site-specific mutagenesis of the hemagglutinin of influenza virus. *J. Cell Biol.* 102:11–23.

Gilson, M. K. 1995. Theory of electrostatic interactions in macromolecules. *Curr. Opin. Struct. Biol.* 5:216–223.

Gray, C., S. A. Tatulian, S. A. Wharton, and L. K. Tamm. 1996. Effect of the N-terminal glycine on the secondary structure, orientation, and interaction of the influenza hemagglutinin fusion peptide with lipid bilayers. *Biophys. J.* 70:2275–2286.

Han, X., D. A. Steinhauer, S. A. Wharton, and L. K. Tamm. 1999. Interaction of mutant influenza virus hemagglutinin fusion peptides with lipid bilayers: probing the role of hydrophobic residue size in the central region of the fusion peptide. *Biochemistry.* 38:15052–15059.

Harter, C., P. James, T. Bachi, G. Semenza, and J. Brunner. 1989. Hydrophobic binding of the ectodomain of influenza hemagglutinin to membranes occurs through the "fusion peptide." *J. Biol. Chem.* 264: 6459–6464.

Hernandez, L. D., L. R. Hoffman, T. G. Wolfsberg, and J. M. White. 1996. Virus-cell and cell-cell fusion. *Annu. Rev. Cell Dev. Biol.* 12:627–661.

Honig, B., and A. Nicholls. 1995. Classical electrostatics in biology and chemistry. *Science.* 268:1144–1149.

Honig, B., K. Sharp, and A. S. Yang. 1993. Macroscopic models of aqueous solutions: biological and chemical applications. *J. Phys. Chem.* 97:1101–1109.

Jacobs, R. E., and S. H. White. 1989. The nature of the hydrophobic binding of small peptides at the bilayer interface: implications for the insertion of transbilayer helices. *Biochemistry.* 28:3421–3437.

Jahnig, F. 1983. Thermodynamics and kinetics of protein incorporation into membranes. *Proc. Natl. Acad. Sci. U.S.A.* 80:3691–3695.

Kessel, A., and N. Ben-Tal. 2000. Free energy determinants of peptide association with lipid bilayers. *In* Peptide-Lipid Interactions. S. A. Simon and T. J. McIntosh, editors. Academic Press, New York.

Kessel, A., D. S. Cafiso, and N. Ben-Tal. 2000a. Continuum solvent model calculations of alamethicin-membrane interactions: thermodynamic aspects. *Biophys. J.* 78:571–583.

Kessel, A., K. Schulten, and N. Ben-Tal. 2000b. Calculations suggest a pathway for the transverse diffusion of a hydrophobic peptide across a lipid bilayer. *Biophys. J.* 79:2322–2330.

Kurumbail, R. G., A. M. Stevens, J. K. Gierse, J. J. McDonald, R. A. Stegeman, J. Y. Pak, D. Gildehaus, J. M. Miyashiro, T. D. Penning, K. Seibert, P. C. Isakson, and W. C. Stallings. 1996. Structural basis for selective inhibition of cyclooxygenase-2 by anti- inflammatory agents. *Nature.* 384:644–648.

Lear, J. D., and W. F. DeGrado. 1987. Membrane binding and conformational properties of peptides representing the NH2 terminus of influenza HA-2. *J. Biol. Chem.* 262:6500–6505.

Luneberg, J., I. Martin, F. Nussler, J. M. Ruysschaert, and A. Herrmann. 1995. Structure and topology of the influenza virus fusion peptide in lipid bilayers. *J. Biol. Chem.* 270:27606–27614.

Macosko, J. C., C. H. Kim, and Y. K. Shin. 1997. The membrane topology of the fusion peptide region of influenza hemagglutinin determined by spin-labeling EPR. *J. Mol. Biol.* 267:1139–1148.

Milik, M., and J. Skolnick. 1993. Insertion of peptide chains into lipid membranes: an off-lattice Monte Carlo dynamics model. *Proteins.* 15: 10–25.

Moll, T. S., and T. E. Thompson. 1994. Semisynthetic proteins: model systems for the study of the insertion of hydrophobic peptides into preformed lipid bilayers. *Biochemistry.* 33:15469–15482.

Nakamura, H. 1996. Roles of electrostatic interaction in proteins. *Q. Rev. Biophys.* 29:1–90.

Ne'methy, G. M., S. Pottle, and H. A. Sheraga. 1983. Energy parameters in polypeptides. 9. Updating of geometrical parameters, nonbonded interactions, and hydrogen bond interactions for the naturally occurring amino acids. *J. Phys. Chem.* 87:1883–1887.

Nicholls, A., and B. Honig. 1991. A rapid finite difference algorithm, utilizing successive over-relaxation to solve the Poisson-Boltzmann equation. *J. Comp. Chem.* 12:435–445.

Nicholls, A., K. A. Sharp, and B. Honig. 1991. Protein folding and association: insights from the interfacial and thermodynamic properties of hydrocarbons. *Proteins.* 11:281–296.

Nozaki, Y., and C. Tanford. 1971. The solubility of amino acids and two glycine peptides in aqueous ethanol and dioxane solutions. Establishment of a hydrophobicity scale. *J. Biol. Chem.* 246:2211–2217.

Picot, D., P. J. Loll, and R. M. Garavito. 1994. The x-ray crystal structure of the membrane protein prostaglandin H2 synthase-1. *Nature.* 367: 243–249.

Sharp, K. A., A. Nicholls, R. F. Fine, and B. Honig. 1991. Reconciling the magnitude of the microscopic and macroscopic hydrophobic effects. *Science.* 252:106–109.

Siegel, D. P., and R. M. Epand. 2000. Effect of influenza hemagglutinin fusion peptide on lamellar/inverted phase transitions in dipalmitoleoylphosphatidylethanolamine: implications for membrane fusion mechanisms. *Biochem. Biophys. Acta.* 1468:87–98.

Sitkoff, D., N. Ben-Tal, and B. Honig. 1996. Calculation of alkane to water solvation free energies using continuum solvent models. *J. Phys. Chem.* 100:2744–2752.

Sitkoff, D., K. Sharp, and B. Honig. 1994. Accurate calculations of hydration free energies using macroscopic solvent models. *J. Phys. Chem.* 98:1978–1988.

Stegmann, T., and A. Heleius. 1993. Influenza virus fusion: from models towards a mechanism. *In* Viral Fusion Mechanisms. J. Bentz, editor. CRC Press, Boca Raton, FL. 89–111.

Steinhauer, D. A., S. A. Wharton, J. J. Skehel, and D. C. Wiley. 1995. Studies of the membrane fusion activities of fusion peptide mutants of influenza virus hemagglutinin. *J. Virol.* 69:6643–6651.

Takahashi, S. 1990. Conformation of membrane fusion-active 20-residue peptides with or without lipid bilayers. Implication of alpha-helix formation for membrane fusion. *Biochemistry.* 29:6257–6264.

Thorgeirsson, T. E., C. J. Russell, D. S. King, and Y. K. Shin. 1996. Direct determination of the membrane affinities of individual amino acids. *Biochemistry.* 35:1803–1809.

Warshel, A., and A. Papazyan. 1998. Electrostatic effects in macromolecules: fundamental concepts and practical modeling. *Curr. Opin. Struct. Biol.* 8:211–217.

White, J. M. 1992. Membrane fusion. *Science.* 258:917–924.

White, S. H., and W. C. Wimley. 1999. Membrane protein folding and stability: physical principles. *Annu. Rev. Biophys. Biomol. Struct.* 28: 319–365.

Wilschut, J., and R. Born. 1993. The influenza virus hemagglutinin: membrane fusion activity in intact virions and reconstituted virosomes. *In* Viral Fusion Mechanisms. J. Bentz, editor. CRC Press, Boca Raton, FL. 133–162.

Wilson, I. A., J. J. Skehel, and D. C. Wiley. 1981. Structure of the haemagglutinin membrane glycoprotein of influenza virus at 3 Å resolution. *Nature.* 289:366–373.

Yang, A. S., and B. Honig. 1995. Free energy determinants of secondary structure formation. I. Alpha-helices. *J. Mol. Biol.* 252:351–365.

Zhou, Z., J. C. Macosko, D. W. Hughes, B. G. Sayer, J. Hawes, and R. M. Epand. 2000. ^{15}N-NMR study of the ionization properties of the influenza virus fusion peptide in zwitterionic phospholipid dispersions. *Biophys. J.* 78:2418–2425.